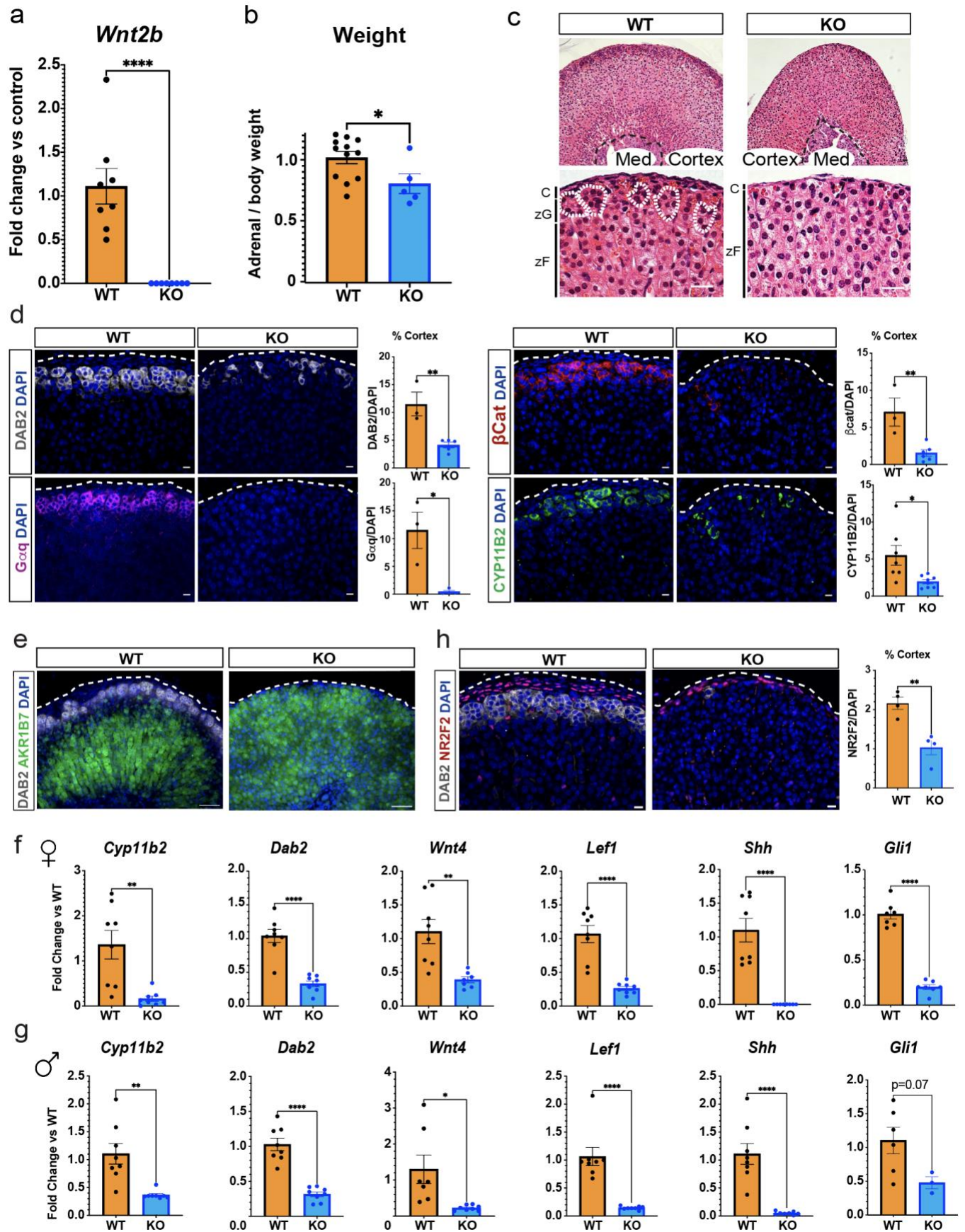
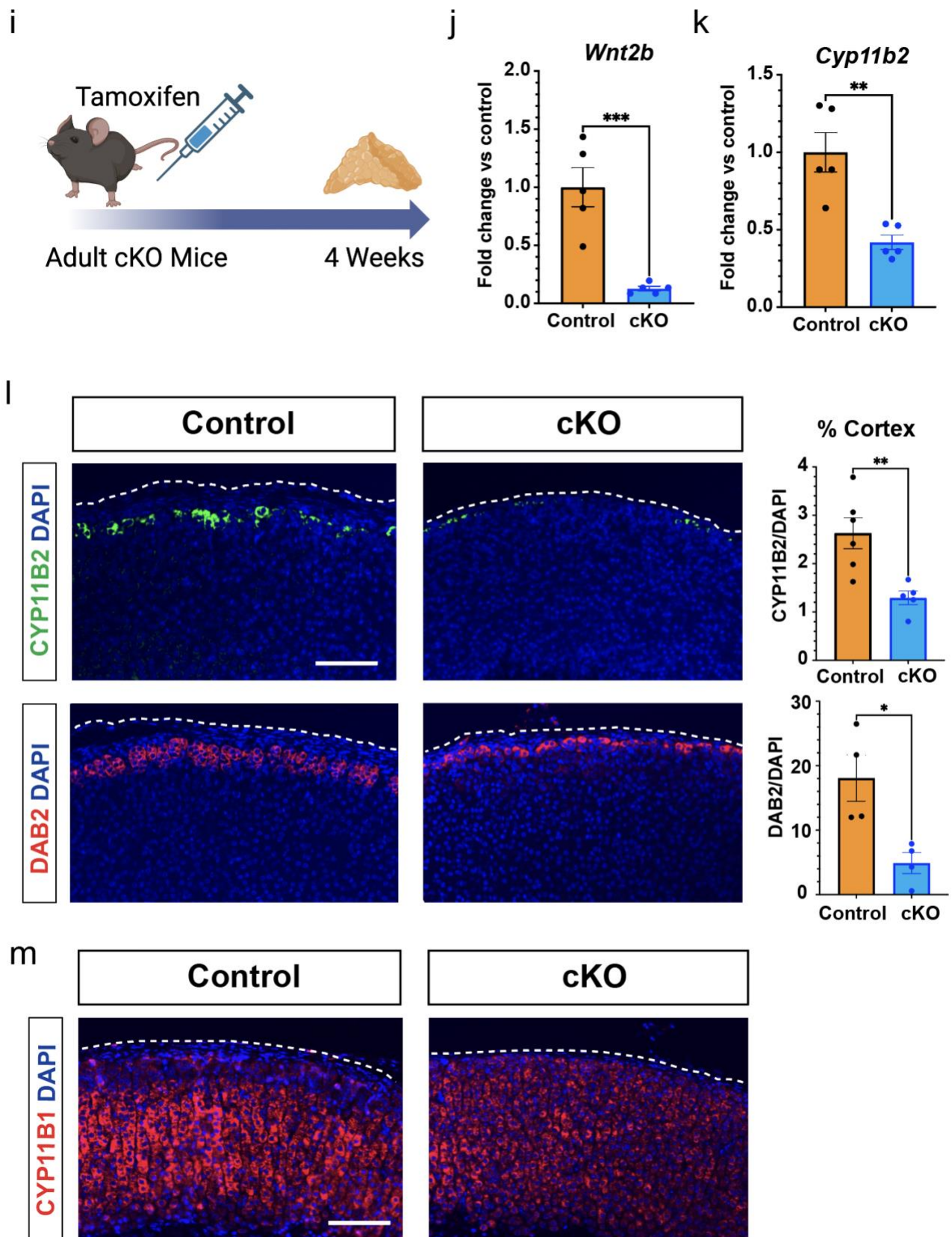


Supplemental Fig. 1



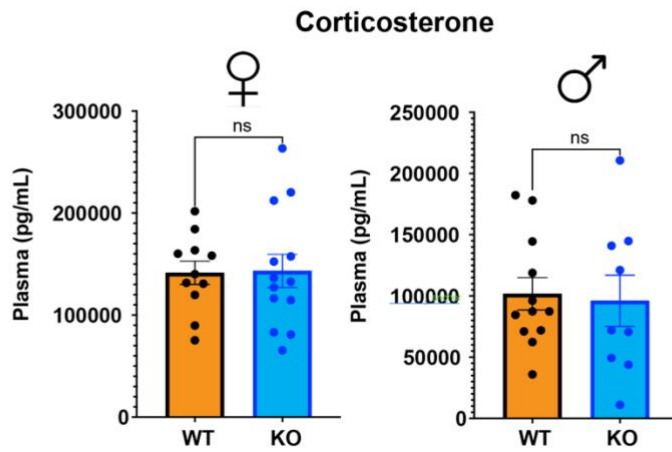
Supplemental Fig. 1



1290 **Supplemental Figure 1. WNT2B deficiency results in a dysmorphic zG in mice.**
1291 a. QRT-PCR was performed on WT and KO male adrenals (n=8 WT, n=8 KO). Two-tailed Student's t-
1292 test. ****p < 0.0001. Data are represented as mean ± SEM.
1293 b. Adrenal weight normalized to body weight from male mice (n=12 WT, n=5 KO). Two-tailed Student's
1294 t-test. *p < 0.05. Data are represented as mean fold change ± SEM.
1295 c. Representative H&E images of WT and KO male adrenals. Scale bar: 10µm. C, capsule; zG, zona
1296 glomerulosa; zF, zona fasciculata; Med, medulla.
1297 d. Representative images and quantification from male adrenals stained for DAB2 (gray, n=3 WT, n=5
1298 KO), Gaq (magenta, n=3 WT, n=4 KO), β-catenin (β-cat, red, n=3 WT, n=6 KO) and CYP11B2 (green,
1299 n=7 WT, n=7 *Wnt2b* KO). Positive cells were quantified and normalized to nuclei (DAPI) in the cortex.
1300 Scale bars: 10µm. Two-tailed Student's t-test. *p < 0.05; **p < 0.01. Data are represented as mean ±
1301 SEM.
1302 e. Representative images stained for DAB2 (gray), AKR1B7 (green) and DAPI (blue) from WT and KO
1303 adrenals. Scale bar: 50µm
1304 f. QRT-PCR was performed on WT and KO female adrenals for *Cyp11b2* (n=8 WT, n=7 KO), *Dab2* (n=8
1305 WT, n=7 KO), *Wnt4* (n=8 WT, n=7 KO), *Lef1* (n=8 WT, n=8 KO), *Shh* (n=8 WT, n=8 KO) and *Gli1* (n=7
1306 WT, n=7 KO). Two-tailed Student's t-test. **p < 0.01; ****p < 0.0001. Data are represented as mean ±
1307 SEM.
1308 g. QRT-PCR was performed on WT and KO male adrenals for *Cyp11b2* (n=8 WT, n=8 KO), *Dab2* (n=8
1309 WT, n=8 KO), *Wnt4* (n=7 WT, n=8 KO), *Lef1* (n=8 WT, n=8 KO), *Shh* (n=8 WT, n=8 KO) and *Gli1* (n=6
1310 WT, n=3 KO). Two-tailed Student's t-test. *p < 0.05; **p < 0.01; ****p < 0.0001. Data are represented as
1311 mean ± SEM.
1312 h. Representative images and quantification of immunostaining for DAB2 (gray) and NR2F2 (red) from
1313 WT and KO adrenals (n=4 WT, n=4 KO). Positive cells were quantified and normalized to nuclei (DAPI,
1314 blue) in the cortex. Scale bars: 10µm. Two-tailed Student's t-test. **p < 0.01. Data are represented as
1315 mean ± SEM.
1316 i. Treatment protocol of adult cKO mice at 6-7 weeks of age with tamoxifen and adrenal harvest after 4
1317 weeks.
1318 j. QRT-PCR was performed for *Wnt2b* in adrenals (n=5 Control and n=5 cKO) 4 weeks following
1319 tamoxifen injection. Two-tailed Student's t-test. ***p < 0.001. Data are represented as mean ± SEM.
1320 k. QRT-PCR was performed for *Cyp11b2* in adrenals (n=5 Control and n=5 cKO) 4 weeks following
1321 tamoxifen injection. Two-tailed Student's t-test. **p < 0.01. Data are represented as mean ± SEM.
1322 l. Representative images and quantification from adrenals stained for CYP11B2 (green, n=6 Control, n=5
1323 cKO and DAB2 (red, n=4 Control, n=4 cKO) 4 weeks following tamoxifen injection. Positive cells were
1324 quantified and normalized to nuclei (DAPI) in the cortex. Scale bar: 100µm. Two-tailed Student's t-test.
1325 *p < 0.05; **p < 0.01. Data are represented as mean ± SEM.
1326 m. Representative images from Control and cKO adrenals stained for CYP11B1 (red) and DAPI (blue)
1327 4 weeks following tamoxifen injection. Scale bar: 100µm.

1328
1329

Supplemental Fig. 2

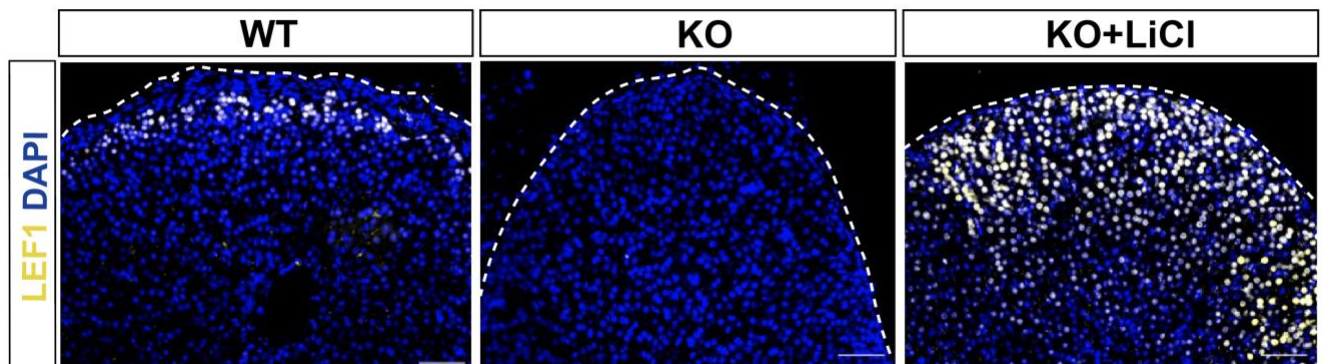


1349
1350
1351
1352
1353
1354
1355
1356

Supplemental Figure 2. WNT2B deficiency does not affect corticosterone levels in mice.

Plasma corticosterone levels (female, n=11 WT, n=13 KO; male, n=12 WT, n=9 KO). Two-tailed Student's t-test. ns, not significant. Data are represented as mean \pm SEM.

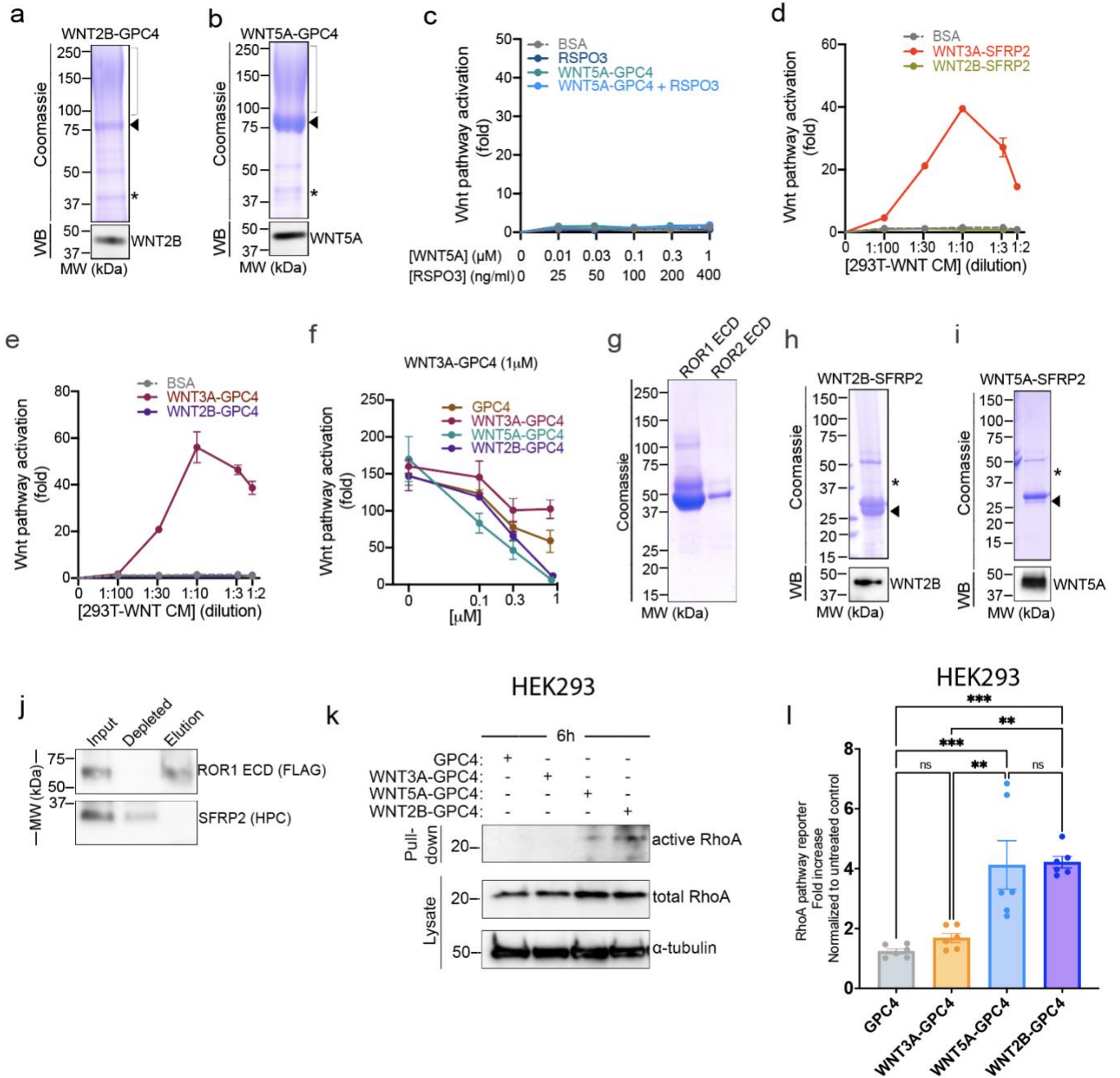
Supplemental Fig. 3



1357
1358
1359
1360
1361

Supplemental Figure 3. Representative images from female adrenals immunostained for LEF1 (yellow) and DAPI (blue) from WT, KO and KO+LiCl mice. Scale bar: 50 μ m

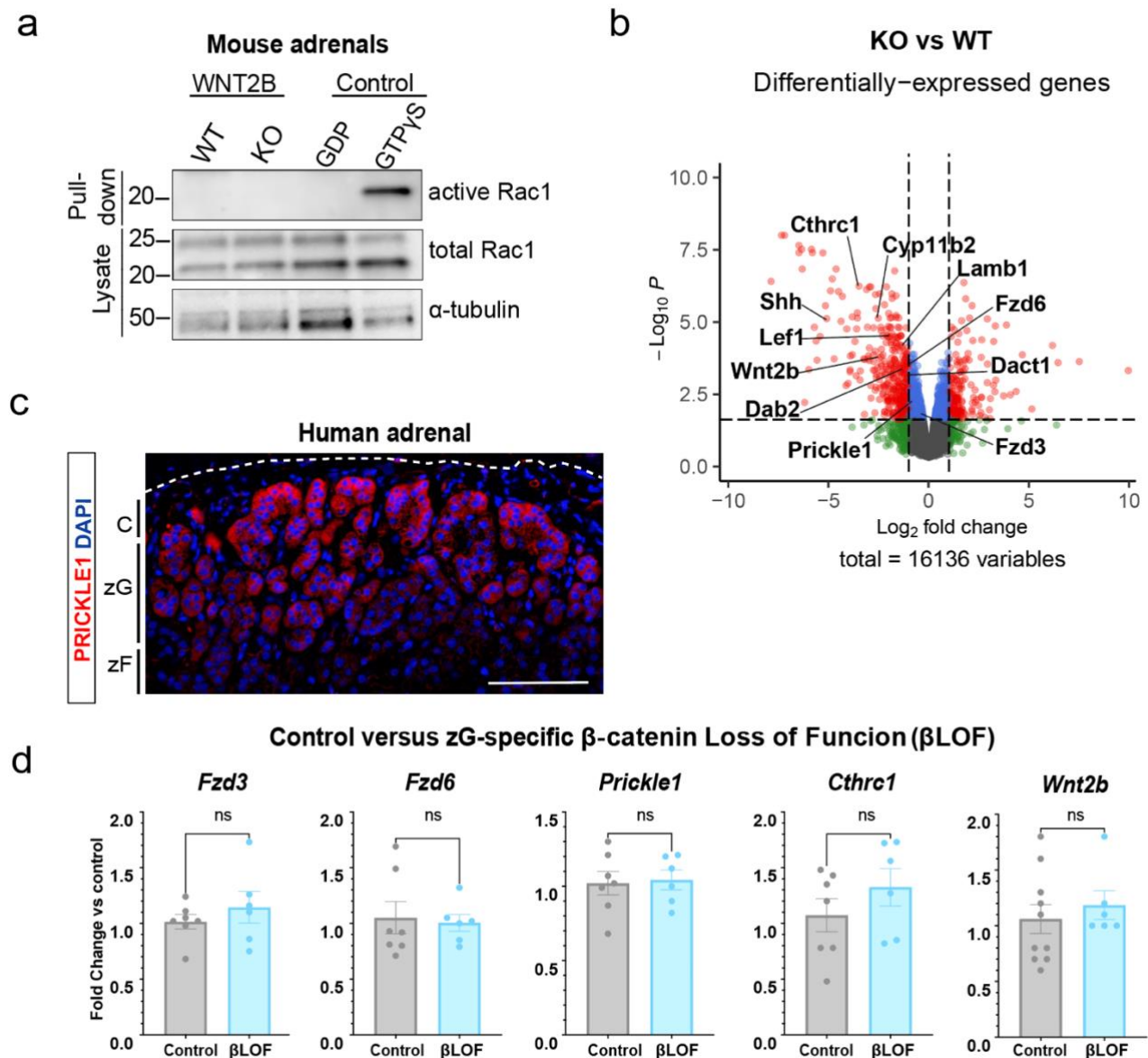
Supplemental Fig. 4



Supplemental Figure 4. Characterization of WNT2B as a non-canonical ligand.

- 1364
1365 a. WNT2B-GPC4 ectodomain, C-terminally tagged with HaloTag7 (HT7) and HPC tag, was affinity
1366 purified from conditioned media on an anti-HPC antibody matrix, and analyzed by SDS-PAGE, followed
1367 by Coomassie staining or anti-WNT2B immunoblotting (WB). Arrowhead indicates unmodified GPC4,
1368 bracket indicates glycosaminoglycan (GAG)-modified species, and asterisks indicate WNT2B protein.
1369 b. As in (a), but with WNT5A in complex with GPC4, and with anti-WNT5A immunoblotting.
1370 c. R-Spondin 3 (RSPO3, 0, 25, 100, 200 and 400ng/ml) or purified WNT5A-GPC4 complex (0.01, 0.03,
1371 0.1, 0.3 and 1 μ M with respect to WNT3A) with or without RSPO3 (400ng/ml) was added to Wnt reporter
1372 cells. After 24h, Wnt pathway activity was measured by luciferase assay. Incubation with BSA served as
1373 negative control. WNT5A-GPC4 does not activate canonical Wnt signaling, even when incubated with
1374 RSPO3. Points represent average activation for two biological replicates, normalized to untreated cells,
1375 and error bars represent SD.
1376 d. SFRP2 (1 μ M) was added in serum-free media in WNT3A- or WNT2B-expressing HEK293 cells. Serial
1377 dilutions of the conditioned media were then added to Wnt reporter cells, and Wnt pathway activity was
1378 measured by Dual-Glo luciferase 24h later. BSA (1 μ M) served as negative control. WNT2B released by
1379 SFRP2 is unable to activate canonical Wnt signaling, in contrast to WNT3A-SFRP2 conditioned media.
1380 Points represent average activation for two biological replicates, normalized to the negative control, and
1381 error bars represent SD.
1382 e. As in (d), but WNT-expressing cells were incubated with 1 μ M of GPC4.
1383 f. As in (Fig. 4d), but purified WNT3A-GPC4 complex (1 μ M) was mixed with the indicated concentrations
1384 of GPC4 alone or in complex with WNT3A, WNT5A or WNT2B. WNT3A-SFRP2 activity is abolished by
1385 WNT5A-GPC4 and WNT2B-GPC4 complexes in a dose-dependent manner, which contrasts GPC4
1386 alone or WNT3A-GPC4 complex.
1387 g. Extracellular domains (ECD) of ROR1 and ROR2, N-terminally tagged with a FLAG tag, were affinity
1388 purified from conditioned media on an anti-FLAG antibody matrix. Purified proteins were analyzed by
1389 SDS-PAGE and Coomassie staining.
1390 h. As in (a), but with WNT2B in complex with SFRP2, C-terminally tagged with 8x-His tag and HPC tag.
1391 i. As in (b), but with WNT5A in complex with SFRP2.
1392 j. Purified SFRP2 (5 μ M) was incubated with FLAG-tagged ROR1-ECD (2.5 μ M), followed by
1393 immunoprecipitation with antibodies against the FLAG tag. Samples were analyzed by SDS-PAGE and
1394 immunoblotting. SFRP2 does not interact with ROR1-Ecd.
1395 k. Activity of RhoA in cell lysates of HEK293 cells treated for 6h with GPC4 alone or in complex with
1396 WNT3A, WNT5A or WNT2B (2 μ M) was assessed by Rhotekin-RBD pull-down assay. RhoA endogenous
1397 levels are shown in the lysates. Both WNT5A-GPC4 and WNT2B-GPC4 complexes induce activity of
1398 RhoA, in contrast to GPC4 alone or in complex with WNT3A. Blotting for α -tubulin served as loading
1399 control.
1400 l. HEK293 cells were co-transfected with the firefly luciferase reporter (pGL4.34) and the renilla luciferase
1401 thymidine kinase reporter (pRL-TK). They were then used to assay RhoA activation by purified GPC4
1402 alone or in complex with WNT3A, WNT5A, and WNT2B (1 μ M). We found that the activity of RhoA is
1403 induced by WNT2B-GPC4 or WNT5A-GPC complexes, but not by WNT3A-GPC4 or GPC4 alone. The
1404 bars represent the average from three independent experiments performed in duplicate, normalized to
1405 untreated cells. Statistical significance was determined using one-way ANOVA with Tukey's post-test
1406 (ns, not significant; **p < 0.01; ***p < 0.001). Data are represented as mean \pm SEM.
1407

Supplemental Fig. 5



1408
1409
1410
1411
1412
1413
1414
1415
1416
1417
1418
1419
1420
1421
1422

Supplemental Figure 5. WNT2B deficiency disrupts Wnt/PCP signaling in the adrenal.

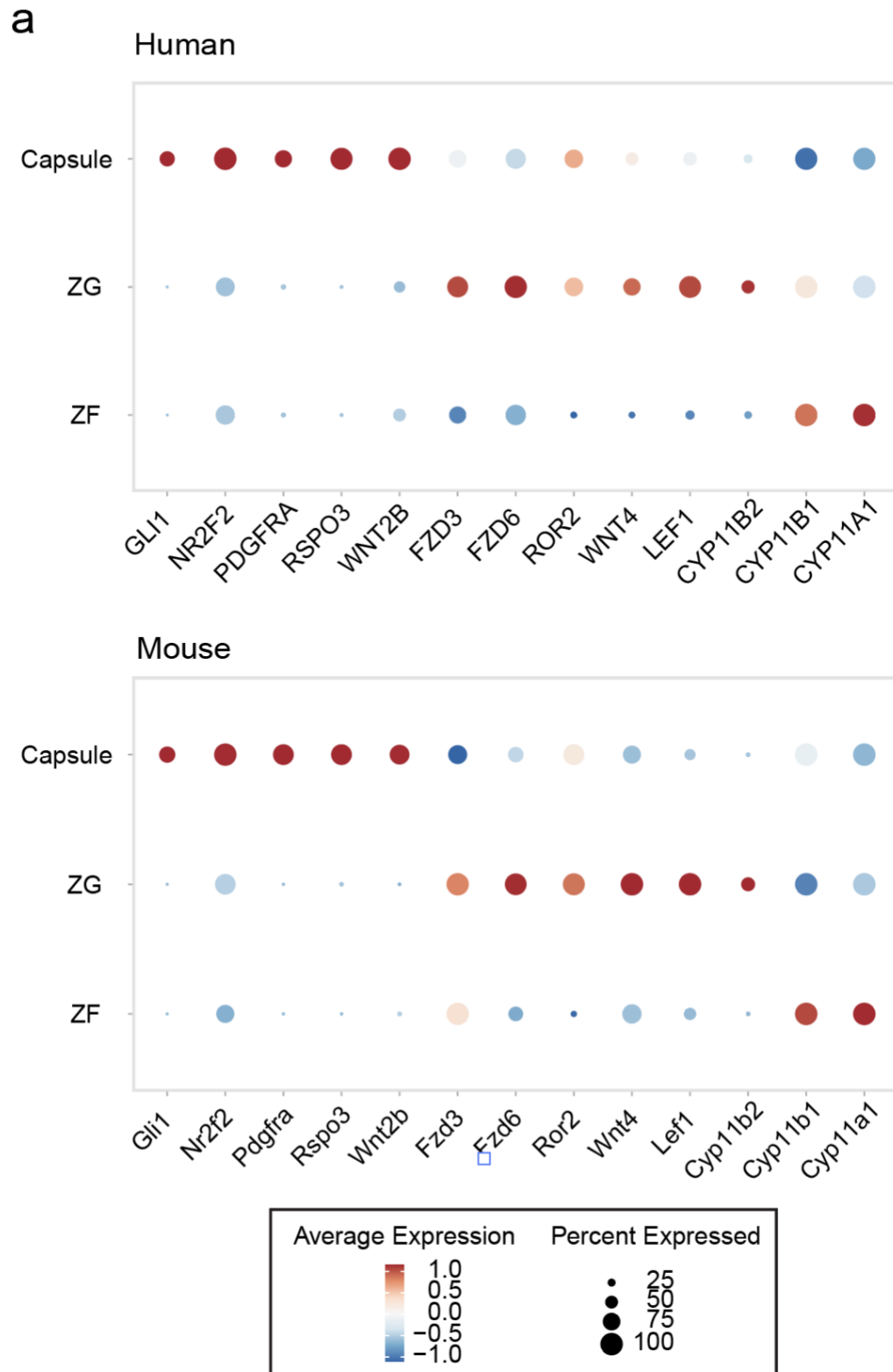
a. Activity of Rac1 in WT and KO adrenals assessed by Rhotekin-RBD pull-down assay using adrenal lysates. GTPγS and GDP treated adrenal lysates served as positive and negative controls, respectively. Total Rac1 and α-tubulin served as loading controls.

b. Volcano plot showing differentially-expressed genes between WT and KO adrenals. Dots representing genes down- and up-regulated in KO are displayed on the left and right sides of the plot, respectively. Red dots represent genes that exhibit a fold-change > 2-fold with a FDR-adjusted p-value < 0.05. Selected zonal markers, including zG genes, are indicated.

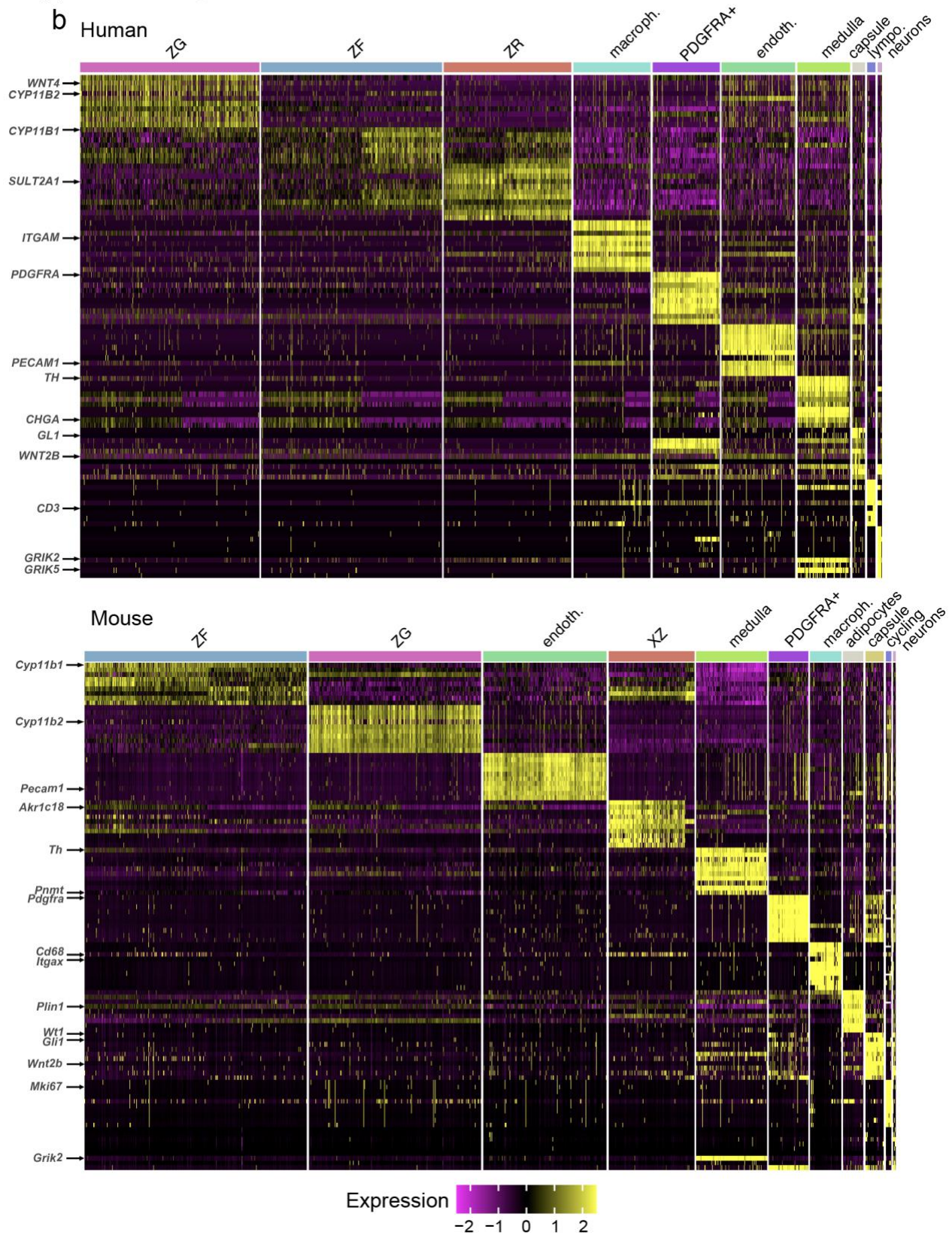
c. Representative image stained for PRICKLE1 (red) and DAPI (blue) from human adrenals. Scale bar: 100μm. C, capsule; zG, zona glomerulosa; zF, zona fasciculata.

d. QRT-PCR was performed in WT and zG-specific β-catenin LOF adrenals for *Fzd3* (n=7 Control, n=6 βLOF), *Fzd6* (n=7 Control, n=6 βLOF), *Prickle1* (n=7 Control, n=6 βLOF), *Cthrc1* (n=7 Control, n=6 βLOF), and *Wnt2b* (n=10 Control, n=6 βLOF). Two-tailed Student's t-test. ns, not significant. Data are represented as mean ± SEM.

Supplemental Fig. 6



Supplemental Fig. 6



1424
1425
1426
1427
1428

Supplemental Figure 6.

a. Dot plot showing average expression of genes in the capsule, zG or zF from human or mouse adrenals.
b. Heatmap visualization showing gene expression patterns of cellular clusters identified in human and mouse adrenals.